



High Precision Straw Tube Chamber With Cathode Readout

V. N. Bychkov, I. A. Golutvin, Yu. V. Ershov, E. V. Zubarev,
A. B. Ivanov, V. N. Lysiakov, A. V. Makhankov, S. A. Movchan,
V. D. Peshekhonov, T. Preda
Joint Institute for Nuclear Research

1992

Abstract:

The high precision straw chamber with cathode readout was constructed and investigated. The 10 mm diameter straws were made of aluminized mylar with transparent longitudinal window. The X coordinate information has been taken from the cathode strips as induced charges and investigated by centroid method. The spatial resolution $\sigma_x = 120 \mu\text{m}$ was obtained at the signal/noise ratio about 60. The possible ways to improve the signal/noise ratio is discussed.

Zubarev

JOINT INSTITUTE FOR NUCLEAR RESEARCH
PARTICLE PHYSICS LABORATORY

HIGH PRECISION STRAW TUBE CHAMBER WITH CATHODE READOUT

V.N.Bychkov, I.A.Golutvin, Yu.V.Ershov, E.V.Zubarev,
A.B.Ivanov, V.N.Lysiakov, A.V.Makhankov, S.A.Movchan,
V.D.Peshekhonov, T.Preda

~~DUBNA~~ 1992

Abstract

The high precision straw chamber with cathode readout was constructed and investigated. The 10 mm diameter straws were made of aluminized mylar with transparent longitudinal window. The X coordinate information has been taken from the cathode strips as induced charges and investigated by centroid method. The spatial resolution $\sigma_x = 120 \mu\text{m}$ was obtained at the signal/noise ratio about 60. The possible ways to improve the signal/noise ratio, is discussed.

1. Introduction

During the last years new modifications of gas coordinate detectors using straw tubes have been investigated and proposed as inner tracking systems for LHC and SSC experiments [1]. The straw chambers have high precision ($\leq 50 \mu\text{m}$), high rate capabilities, short memory time and can work with high pressure up to 4 atm. They can be industrially produced and used also as a part of large-scale muon detecting systems.

In this paper we present characteristics of the straw chamber with mylar straws and cathode readout which combines to some extent properties of the drift chambers [2], drift metal tubes [3], honeycomb chambers with cathode readout [4].

2. The chamber construction

The scheme of the chamber is shown in fig.1. It consists of a set of mylar straws fixed to the fiberglass support. On the upper surface of the support there are copper strips, orthogonal to straws. Thickness of fiberglass plane and copper strips is 2.5 mm and $50 \mu\text{m}$ respectively. Strip pitch ($a+b$) is 3, 4 or 5 mm and interval value b is 0.5, 0.5 or 1mm, respectively. The length of the strips was 1 m.

The straws, 10 mm in diameter with longitudinal seam, were made of the aluminized mylar $25 \mu\text{m}$ thick processed by ultrasonic welding. In our construction the straws with aluminiumless longitudinal windows facing toward the strips have been used. The gold plated tungsten wires are kept with 200 grams tension in the center of the straw. The wire diameters are $50 \mu\text{m}$. The tube body tension is 100 grams.

With this chamber one can determine Y-coordinates of the charged particle tracks by drift time measurement, and X-coordinates by processing the charges which are induced by avalanches on the strips through the transparent window.

The maximum value of the window angle, $2 \times \varphi$, is limited by the value of the accumulated electrical charge. Fig. 2 gives the dependence of the relative anode signal on the window size. The measurements were done with 8 KeV X-ray beam of 1 mm in diameter. The beam intensity was $2 \times 10^4 \text{ cm}^{-2} \text{ s}^{-1}$ and the gas gain was about 2×10^5 . For window angles more than 36° the anode signal drops very fast. This size was chosen for further measurements.

The distribution of the induced charge in X-direction is given in fig. 3 for 13 k Ω and 200 k Ω input resistance of the charge amplifiers. The total width of the distribution (FWTM) is almost independent of the input resistance and is about 3R, where R is the straw radius. Together with [6], we conclude that the optimum strip pitch should be equal to R for the best spatial resolution.

Figure 4 shows the distribution of the induced signals on a 200 μm diameter wire moving parallel to the anode wire in front of the transparent window. The angle ϑ has vertex on the anode wire and $\vartheta=0$ corresponds to the middle of the window. The width of the distribution (FWTM) corresponds to the window size.

4. The spatial resolution

The spatial resolution of the chamber has been investigated using the X-rays collimated beam moving with good accuracy in X and Y directions. The beam diameter was less than 100 μm (FWHM). The signals from the strips through the charge-sensitive amplifier were transported to the TDC and then to PC computer. The anode signals trigger the system. The amplifier parameters are:

- input resistance is 13 k Ω ;
- voltage-charge conversion coefficient is 6.7 V/pC;
- noise is 3×10^{-3} pC (6 σ);
- integrating time is 60 ns.

The gas mixture was Ar/CH₄(50/50).

The spatial resolution is determined by centroid [6,7] and charge-ratio methods [4] using charge read out from

three neighbouring strips and described in a separate paper [5]. The best value of the spatial resolution, σ , presented below has been obtained for the 5 mm strip pitch (the 1m length strip had capacity about 300 pF).

We have obtained the spatial resolution, σ , fitting the event distributions measured with the different signal/noise ratios. An example of these distributions is shown in fig. 5.

Figure 6 presents the dependence of the spatial resolution on the signal/noise ratio for the avalanche position near the center of the strip. We have checked that it is rather independent on the avalanche position across the strips. One can see from fig. 6 that the spatial resolution almost linearly depends on the signal/noise ratio. The best resolution of $(103 \pm 4) \mu\text{m}$ is obtained at the signal/noise ratio of about 70. This can be further reduced using higher signal/noise ratios. There are several ways to improve this ratio probably by factor two [8]:

- using low-noise electronics;
- working with higher gas gain (in the saturated proportional mode and limited streamer mode);
- using the mylar straws with carbon covering the window.

5. Conclusion

In conclusion we have constructed and investigated characteristics of the straw chamber with cathode strip readout.

The spatial resolution of $(103 \pm 4) \mu\text{m}$ was obtained with the signal/noise ratio at about 70. This value is good enough for a single layer of the LHC/SSC muon detector.

The authors express their gratitude to V.S. Khabarov for his help during the work and Z.I. Smirnova for assembling quality.

1. Walter H.Toki. SLAC - PUB - 5332 (1990).
2. B.Adeva, M.Aguilar-Benitez, H.Akbari et al. Nucl.Instr.and Meth. in Physics Research A289 (1990) 35.
3. GEM. Letters of Intent.
4. H.van der Graaf, J.Buskens, G.Faber et al. Nucl.Instr.and Meth. in Physics Research A307 (1991) 220.
5. I.A. Golutvin, S.A. Movchan, V.D. Peshekhonov, T. Preda, to be published in Nucl. Instr. and Meth.
6. I.Endo, T.Kawamoto, Y.Mizuno et al. Nucl.Instr.and Meth. 188 (1981) 51.
7. J.Chiba, H.Iwasaki, T.Kageyama et al. Nucl.Instr.and Meth. 206 (1983) 451.
8. V.D.Peshekhonov. Wire Chamber Conference 1992, Viena, Austria (February, 1992) (to be published).

FIGURE CAPTIONS

- Fig.1. The scheme of the chamber (at right) and the straw (at left).
- Fig.2. The dependence of the relative anode signal on window angle.
- Fig.3. The spatial distribution of induced charge value on X-coordinate.
- Fig.4. The induced charge distribution across the straw window.
- Fig.5. The event distribution as a function of the avalanche position measured with signal/noise ratio of about 60. The solid line is gaussian fit.
- Fig.6. The detector spatial resolution dependence on signal/noise ratio.

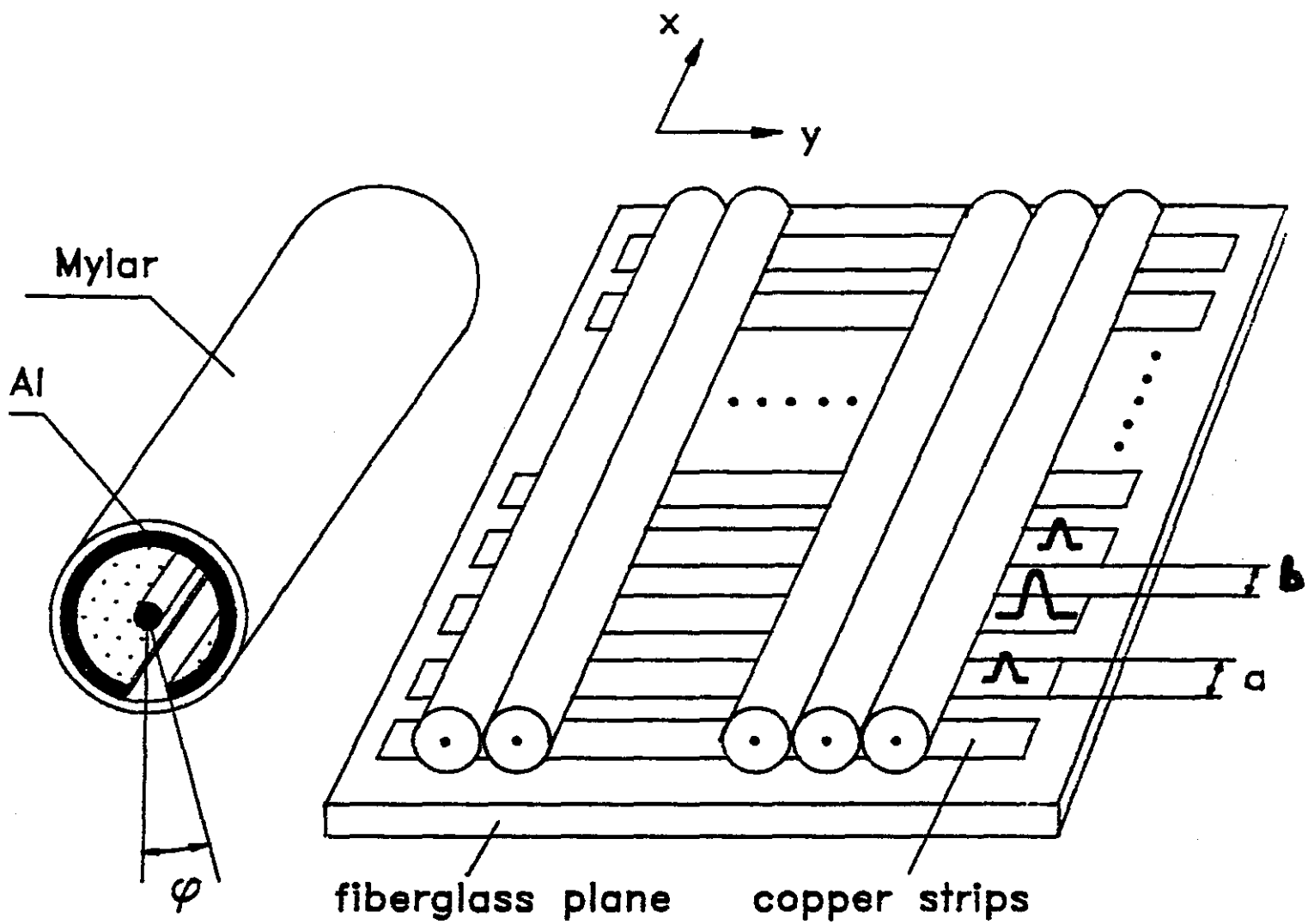


Fig. 1

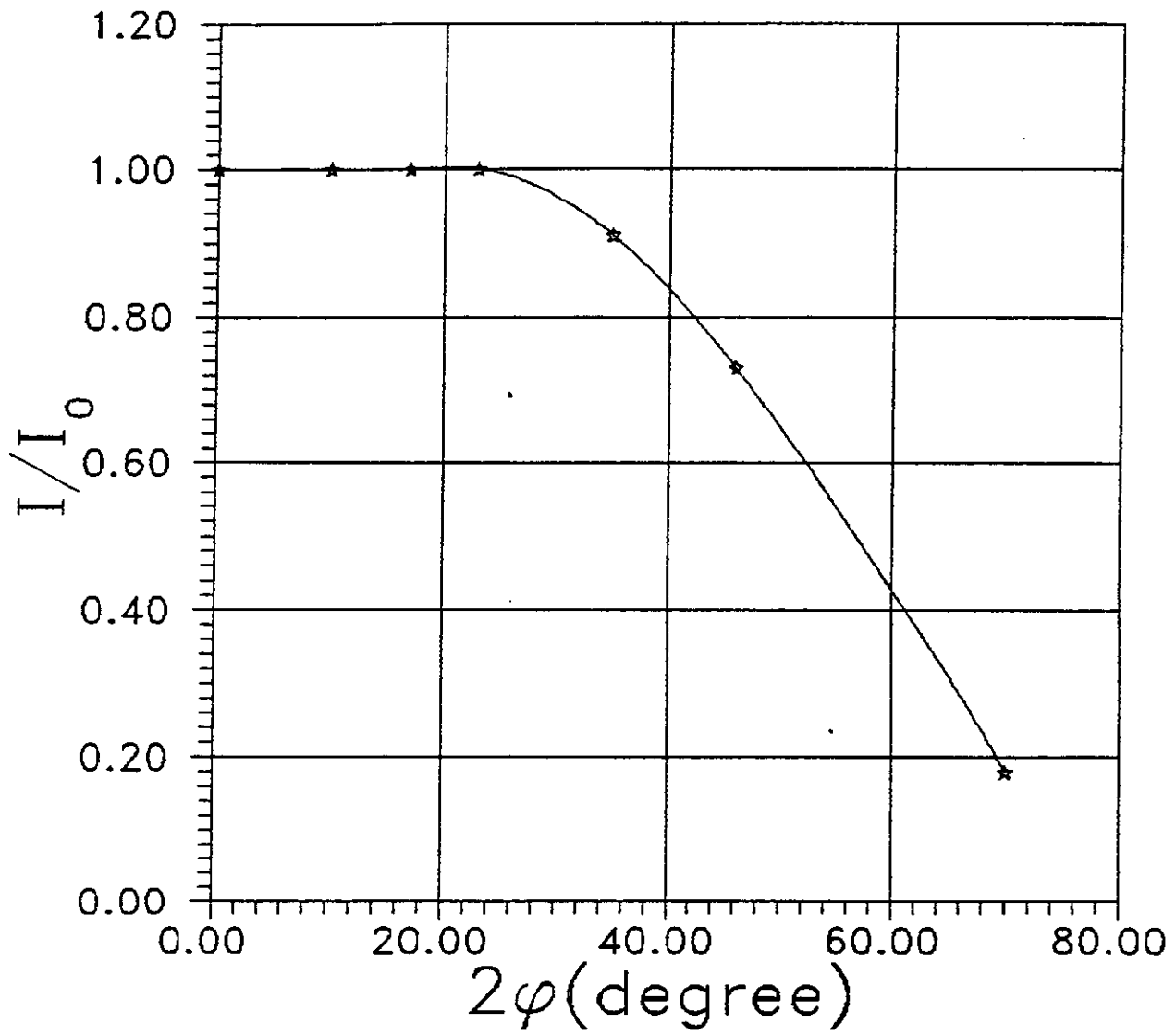


Fig. 2.

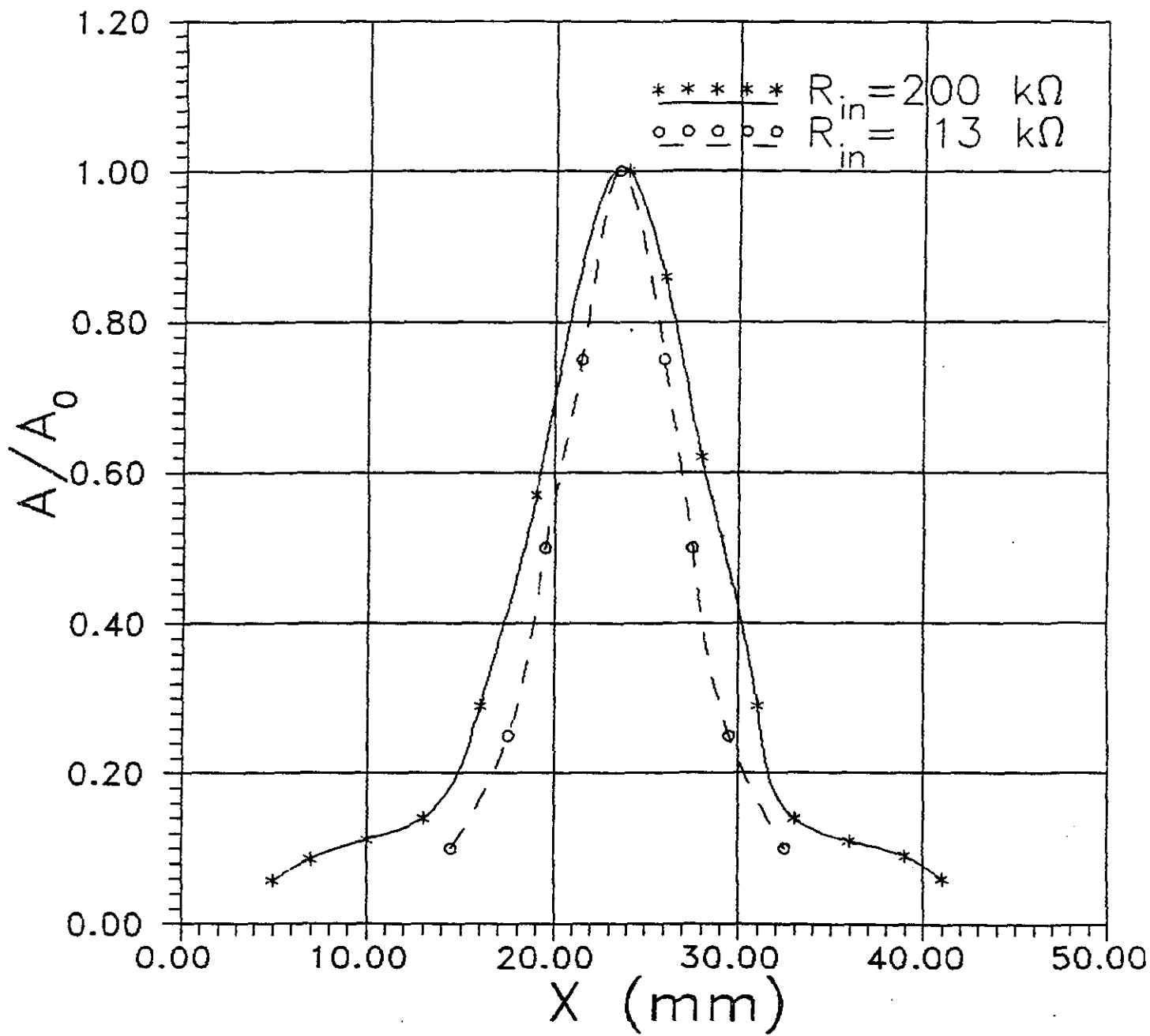


Fig. 3.

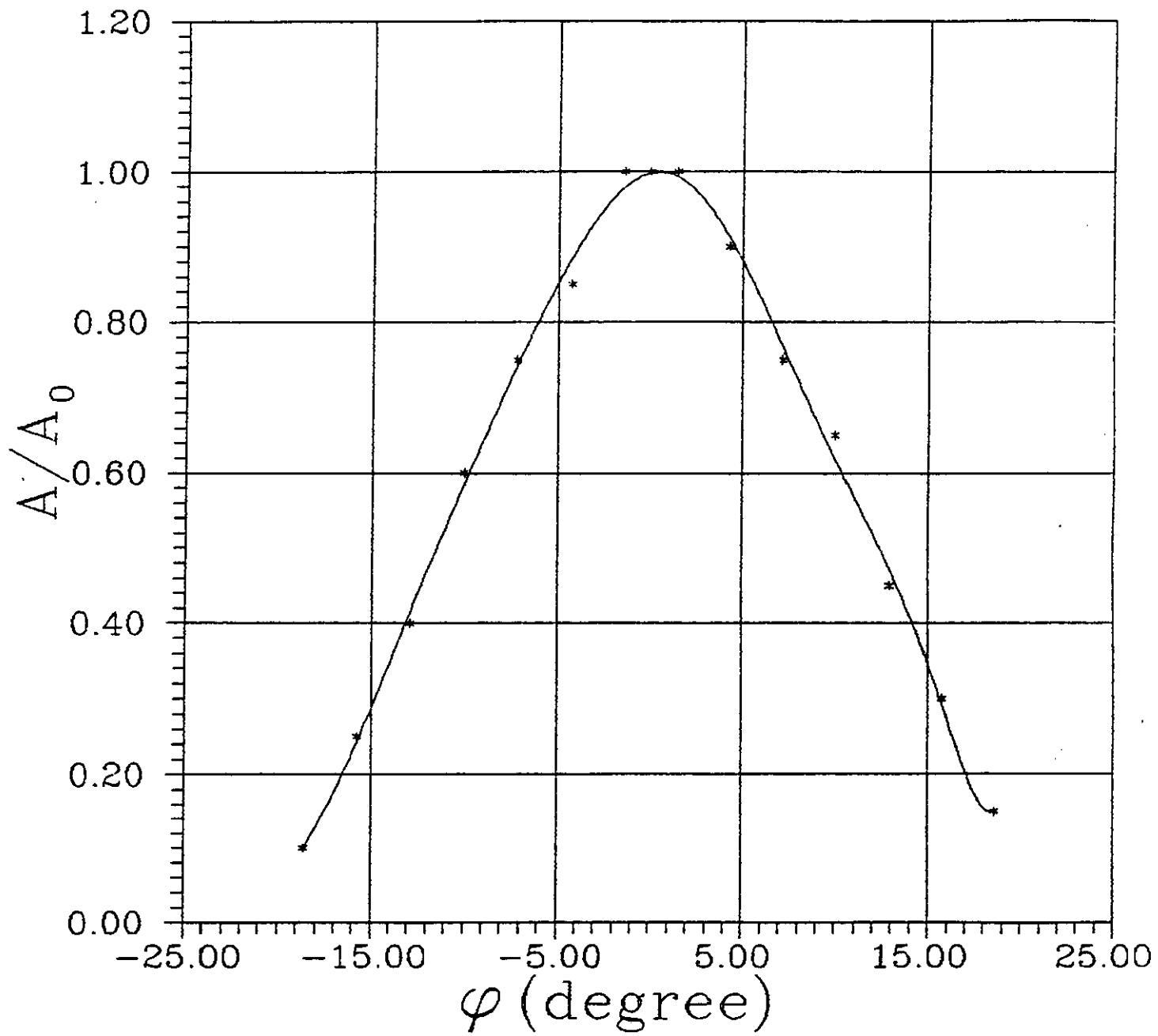


Fig. 4.

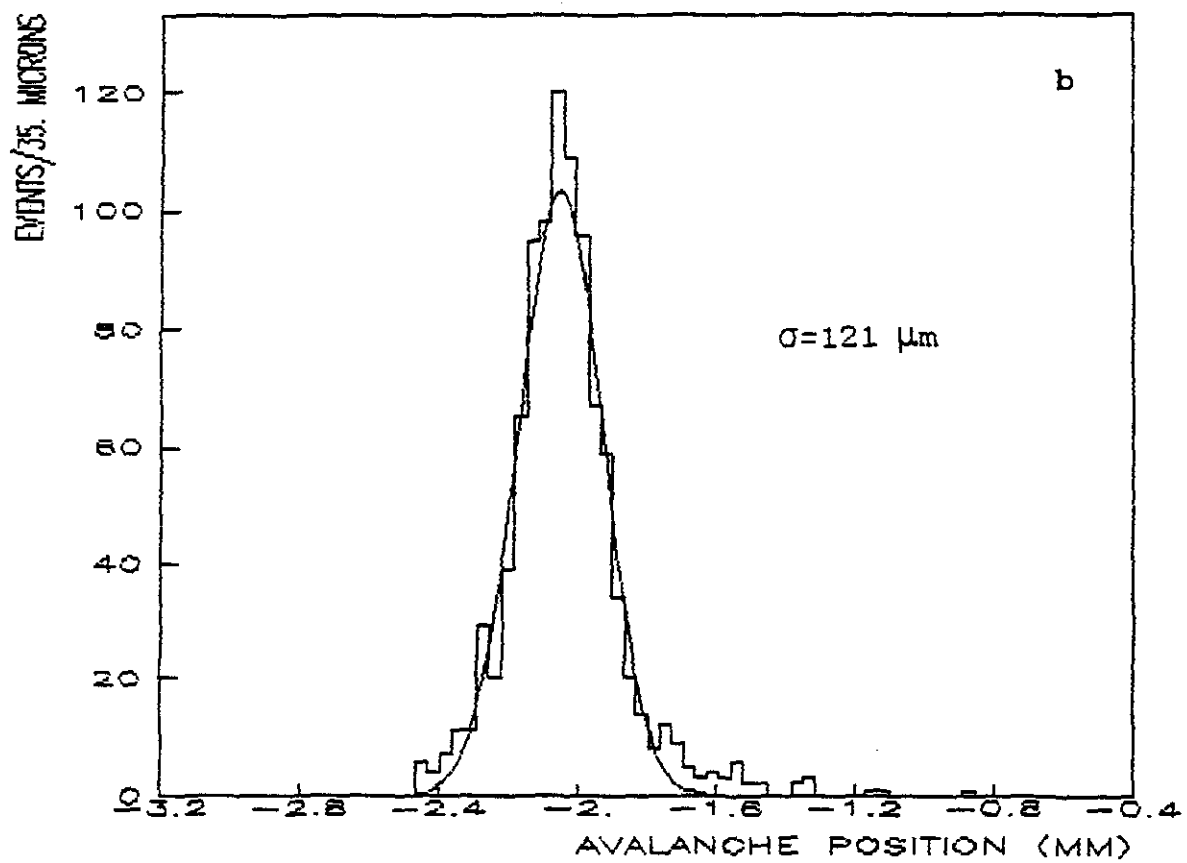
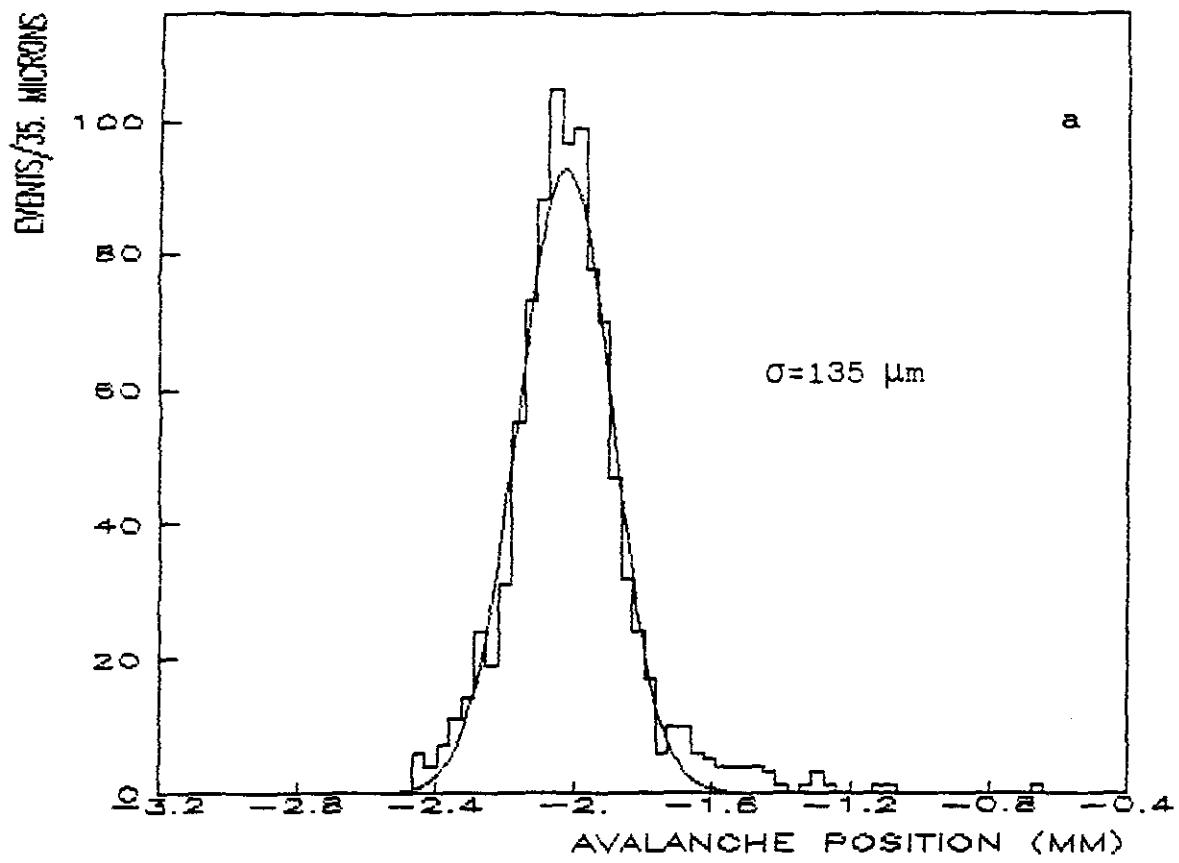


Fig. 5

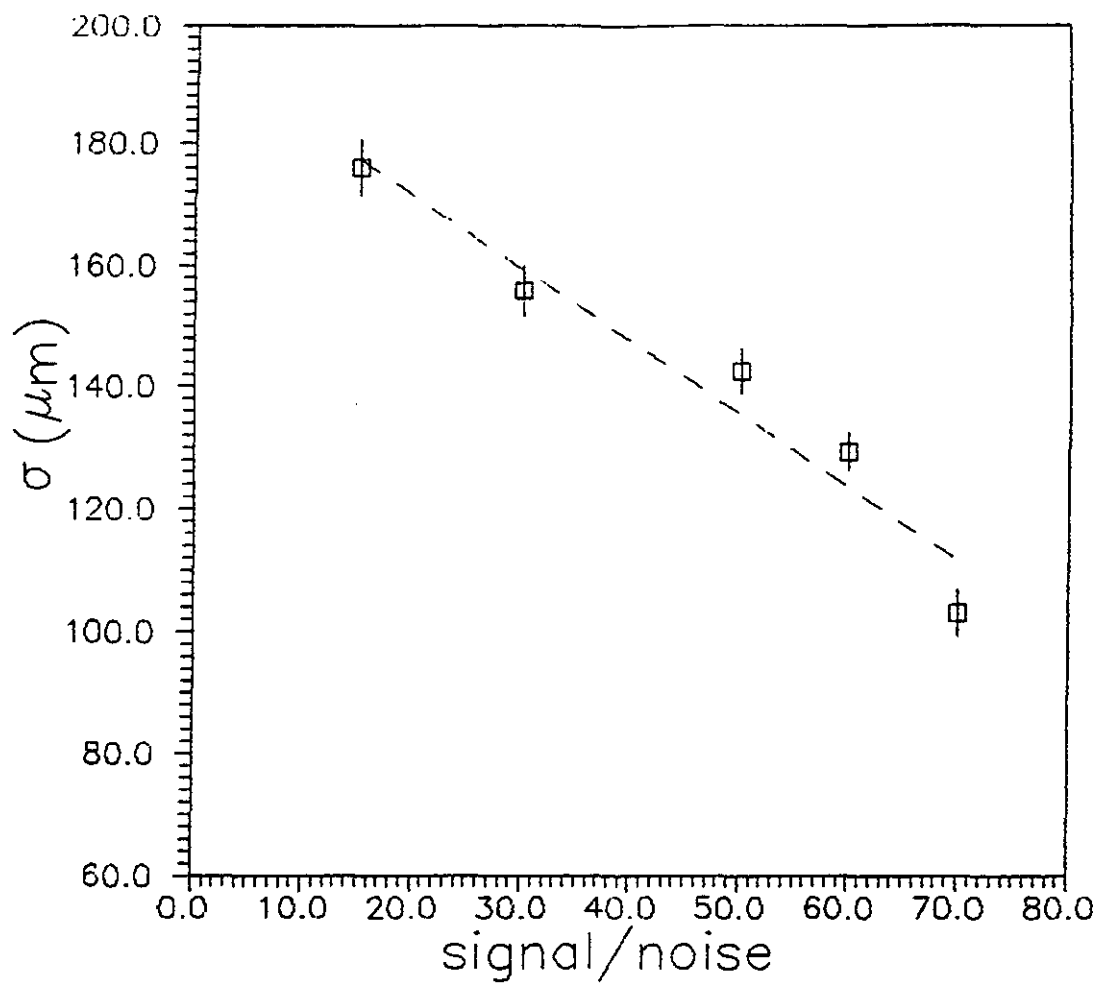


Fig 5